ELSEVIER

Modelling of periodic wave transformation in the inner surf zone

P. Bonneton

Department of Geology and Oceanography, UMR CNRS EPOC, University of Bordeaux I, 33405 Talence, France

Abstract

In this paper, we analyse the ability of the nonlinear shallow-water (NSW) equations to predict wave distortion and energy dissipation of periodic broken waves in the inner surf zone. This analysis is based on the weak-solution theory for conservative equations. We derive a new one-way model, which applies to the transformation of non-reflective periodic broken waves on gently sloping beaches. This model can be useful to develop breaking-wave parameterizations (in particular broken-wave celerity expression) in both time-averaged wave models and time-dependent Boussinesq-type models. We also derive a new wave set-up equation which provides a simple and explicit relation between wave set-up and energy dissipation. Finally, we compare numerical simulations of both, the NSW model and the simplified one-way model, with spilling wave breaking experiments and we find a good agreement.
© 2006 Elsevier Ltd. All rights reserved.

Keywords: Surf zone; Broken wave; Bore; Shock; Nonlinear shallow-water equations; Saint Venant equations; One-way equation; Weak solution; Energy dissipation; Wave set-up

1. Introduction

The dominant types of breakers in natural sandy beaches are spilling and plunging breakers (Galvin, 1968). In both cases, immediately after the initiation of breaking a rapid change in the wave shape occurs, in a region that has been named the "transition region" (Svendsen et al., 1978). Shoreward of this region the wave field changes more slowly and reorganizes itself into quasi-periodic bore-like waves. This region, which extends to the shoreline where the run-up starts, has been termed the "inner surf zone" (ISZ). In this paper we consider conditions for which the surf zone has a significant ISZ, and then beaches of sufficiently gentle uniformly varying slopes. For these conditions, nonlinear shallow-water (NSW) equations are a good approximation to wave motion (e.g. Kobayashi et al., 1989; Liu et al., 1991). Following the concept of "weak solutions" (Whitham, 1974), the ISZ broken-wave solution can be approximated by representing wavefronts as discontinuities. The NSW weak-solution approach, extensively used in hydraulics problems (Stoker, 1957; Whitham, 1974) has been successfully applied for studying single bore

propagation on a beach. For instance, one-way analytical solutions of this phenomenon were first given by Whitham (1958) and Ho and Meyer (1962), and numerical simulations were performed by Keller et al. (1960) and Hibbert and Peregrine (1979). On the other hand, only few theoretical NSW-based studies have been devoted to the dynamics of periodic broken waves in the ISZ. However, numerical studies (e.g. Kobayashi et al., 1989, 1990; Cox, 1995; Bonneton, 2003) have shown that shock-capturing numerical NSW models give good results in comparison with laboratory measurements of periodic broken waves.

In the present paper, we derive a new one-way model, based on the NSW equations, which applies to the transformation of non-reflective periodic broken waves on gently sloping beaches. Even if numerical solutions of the complete NSW equations can be computed, our simplified one-way approach is useful because it gives us a better understanding of wave distortion and energy dissipation in the ISZ. Moreover, this one-way approach can be useful to provide breaking-wave parameterizations (in particular broken-wave celerity expression) in both time-averaged wave models and time-dependent Boussinesq-type models. In this paper, we also derive a new set-up equation based on the NSW weak-solution theory.

E-mail address: p.bonneton@epoc.u-bordeaux1.fr.

This equation is interesting from a physical point of view because, contrary to the classical approach based on radiation stresses, it provides a simple and explicit relation between wave set-up and energy dissipation in the surf zone.

The paper is outlined as follows. In Section 2, we briefly introduce the NSW weak-solution theory. From this approach we derive both a new one-way model (Section 3) and a new wave set-up expression (Section 4). Finally in Section 5, validity of both NSW and one-way models is assessed from comparisons with laboratory ISZ experiments.

2. Governing equations

The NSW equations with friction (also named Saint Venant equations) are a good approximation to wave motion in the surf zone of gently sloping beaches. The one-dimensional NSW equations are given by

$$\frac{\partial h}{\partial t} + \frac{\partial hu}{\partial x} = 0, \tag{1}$$

$$\frac{\partial hu}{\partial t} + \frac{\partial}{\partial x}\left(hu^2 + \frac{1}{2}gh^2\right) = gh\frac{\partial d}{\partial x} - \frac{\tau_b}{\rho}, \tag{2}$$

where x is the horizontal coordinate, u is the depth-averaged cross-shore velocity, h is the total water depth, d is the bed elevation, g is the gravitational acceleration and τ_b the bottom-shear stress. The wave elevation ζ is given by $\zeta = h - d$. We use a standard bottom friction parameterization: $\tau_b = \frac{1}{2}\rho f_r |u|u$, where f_r is the friction coefficient.

Following the concept of "weak solutions" (Whitham, 1974), we can approximate the ISZ broken-wave solution (Fig. 1a) by introducing a discontinuity (see Fig. 1b) satisfying jump conditions based on mass and momentum conservation across the shock:

$$-c_b[h] + [hu] = 0,$$

$$-c_b[hu] + [hu^2 + \tfrac{1}{2}gh^2] = 0,$$

where the brackets [ ] indicate a jump in the quantity and c_b is the shock velocity. A conventional notation is to use subscript 1 and 2 for values ahead and behind the shock,

respectively (see Fig. 1b). So the jump conditions may also be written in the form

$$u_1 - c_b = -\left(\frac{gh_2}{2h_1}(h_2 + h_1)\right)^{1/2}, \tag{3}$$

$$u_2 - c_b = -\left(\frac{gh_1}{2h_2}(h_2 + h_1)\right)^{1/2}. \tag{4}$$

Mathematically, the composite solution, composed of continuously differentiable parts satisfying Eqs. (1) and (2), together with jump conditions (3), (4), can be considered a weak solution of the NSW equations.

The energy of the NSW weak solution is not conserved in presence of shocks. Following Stoker (1957), the energy dissipation D_b across a shock is given by $D_b = -[\mathscr{F}] + c_b[\mathscr{E}]$, where $\mathscr{E} = \frac{1}{2}\rho(hu^2 + g(\zeta^2 - d^2))$ is the energy density and $\mathscr{F} = \rho hu(\frac{1}{2}u^2 + g\zeta)$ is the energy flux density. Using jump conditions (3) and (4), the broken-wave energy dissipation can be expressed as

$$D_b = \frac{\rho g}{4}\left(\frac{g(h_2 + h_1)}{2h_1 h_2}\right)^{1/2}(h_2 - h_1)^3 \tag{5}$$

or, equivalently,

$$D_b = \frac{\rho g}{4}\frac{|Q_b|}{h_1 h_2}(h_2 - h_1)^3, \tag{6}$$

where $Q_b = h_1(u_1 - c_b) = h_2(u_2 - c_b)$ is the volume flux across the shock in the coordinate system moving with the broken-wave celerity c_b.

Expression (6) is often used in the coastal-engineering literature, but generally it is introduced from an analogy between an ISZ broken wave and a hydraulic jump (e.g. Le Méhauté, 1962; Battjes and Janssen, 1978; Svendsen et al., 1978, 2003). However, the hydraulic jump is a special case of "shock wave" where the energy dissipation remains constant over time. It is worthwhile to note that the broken-wave dissipation given by Eq. (6) can be applied to any shallow-water broken wave, even to non-saturated breakers ($H > h_2 - h_1$, e.g. Fig. 1), and not only to hydraulic jumps or fully developed bores.

3. A one-way broken-wave model

The motion of a single bore propagating into water at rest on a beach has been studied for a long time. One-way analytical solutions of this phenomenon were first given by Whitham (1958) and Ho and Meyer (1962), and numerical simulations were performed by Keller et al. (1960) and Hibbert and Peregrine (1979). On the other hand, only few studies have been devoted to the propagation of periodic broken waves on a gently sloping beach. This is mainly due to the fact that jump conditions at a wavefront are more complex for periodic broken waves (velocity ahead the wavefront, u_1, is a negative unknown quantity) than for a single bore which propagates into quiescent water ($u_1 = 0$).
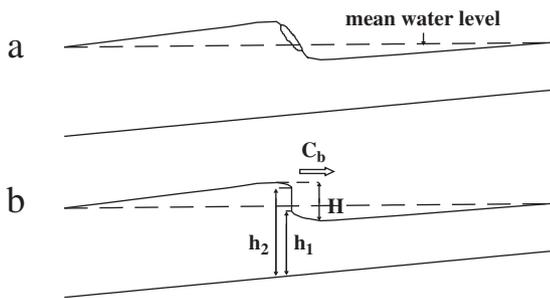

Fig. 1. Definition sketch. (a) Cross-section of a broken wave in the ISZ. (b) Shock representation. c_b is the broken-wave celerity, H the wave height, h the water depth and subscripts 1 and 2 indicate values, respectively, ahead and behind the shock.

In this section, we present a simplified one-way version of the NSW model, which applies to the transformation of non-reflective periodic broken waves on gently sloping beaches. Even if wave reflexion in the field can be significant, a simplified one-way approach is useful for nearshore applications. Indeed, breaking-wave parameterizations in both time-averaged wave models (e.g. Svendsen et al., 2003) and time-dependent Boussinesq-type models (e.g. Madsen et al., 1997) are based on one-way approaches. In particular, a key point of these parameterizations is the estimation of the broken-wave celerity from a one-way model (see Bonneton, 2004).

We first consider the case of wave propagation on a horizontal bottom. Such a situation represents an interesting limiting case of wave propagation on a gently sloping beach, even if in this case dispersive mechanisms actually play a significant role. If the still water depth is constant, $d = d_0$, and the friction term is discarded, the hyperbolic system of equations (1) and (2) may be expressed by two characteristic equations,

$$\left\{ \frac{\partial}{\partial t} + (u \pm c)\frac{\partial}{\partial x} \right\}(u \pm 2c) = 0, \tag{7}$$

where $c(h) = (gh)^{1/2}$. The Riemann invariants $\alpha^{\pm} = u \pm 2c$ are constant along characteristic curves $C^{\pm}$ defined by $dx/dt = u \pm c$.

The weak-solution theory becomes particularly simple in the case of problems in which the wave field has one of the Riemann invariants constant throughout. A wave solution corresponding to such a situation is called a "simple wave" (see Stoker, 1957). For instance, if a wave is propagating in the positive x-direction into water of constant depth d_0 and constant velocity u_0, α^- is constant and is given by

$$\alpha^- = u - 2c = u_0 - 2c_0 \tag{8}$$

with $c_0 = (gd_0)^{1/2}$. Consequently, the two NSW equations reduce to a one-way equation which is either the mass conservation equation

$$\frac{\partial h}{\partial t} + \frac{\partial q(h)}{\partial x} = 0 \tag{9}$$

or the momentum conservation equation

$$\frac{\partial q(h)}{\partial t} + \frac{\partial}{\partial x}(q(h)^2/h + 0.5gh^2) = 0, \tag{10}$$

where $q(h) = hu = h(u_0 - 2c_0 + 2c(h))$. These two equations are equivalent provided that the wave solution is continuous. However, when a shock is involved, this equivalency no longer holds, because there is a jump in α^- quantity at the shock. This jump, $[\alpha^-]$, can be obtained by subtracting Eq. (4) from Eq. (3). We find

$$[\alpha^-] = -2(g(h_1 + h_2)/2)^{1/2}$$
$$\times \left(\frac{\varepsilon}{(1 - \varepsilon^2)^{1/2}} - (1 + \varepsilon)^{1/2} + (1 - \varepsilon)^{1/2} \right), \tag{11}$$

where $\varepsilon = (h_2 - h_1)/(h_2 + h_1)$ is the shock strength. Laboratory observations of monochromatic waves on planar

beaches (e.g. Bowen et al., 1968; Svendsen et al., 1978) and field measurements (e.g. Thornton and Guza, 1982; Raubenheimer et al., 1996; Sénéchal et al., 2001) show that the order of magnitude of ε is about 0.3. Bonneton (2001) has shown that for such moderate shock strength neglecting changes in the Riemann invariant α^- constitutes a reasonable approximation, and so Eq. (8) can be applied even at a shock.

This approximation allows the one-way Eq. (9) to be retained and combined with the jump condition, $-c_{b_s}[h] + [q(h)] = 0$, which yields the relation

$$c_{b_s} = u_0 - 2c_0 + 2g^{1/2}\frac{h_2^{3/2} - h_1^{3/2}}{h_2 - h_1}, \tag{12}$$

where c_{b_s} is the one-way shock celerity. The energy dissipation D_{b_s} is given by $D_{b_s} = -[\mathscr{F}] + c_{b_s}[\mathscr{E}]$, which leads to

$$D_{b_s} = \frac{\rho}{g}(c_2 - c_1)^3$$
$$\times \left(c_2^2 + 3c_1c_2 + c_1^2 + (u_0 - 2c_0)\frac{(c_2^2 + 4c_1c_2 + c_1^2)}{2(c_2 + c_1)} \right) \tag{13}$$

with $c_1 = c(h_1)$ and $c_2 = c(h_2)$. Celerity c_{b_s} and dissipation D_{b_s} are approximations of the exact shock celerity c_b and dissipation D_b. Fig. 2 presents the relative errors $(c_b - c_{b_s})/c_{b_s}$ and $(D_b - D_{b_s})/D_{b_s}$ in function of the shock strength ε, assuming that $(h_2 + h_1)/2/d_0 \sim 1$ and $u_0 = 0$. This figure shows that, even if c_{b_s} and D_{b_s} are smaller than c_b and D_b, they represent good approximations when the shock is of moderate strength, as in the case of ISZ broken waves.

Let us consider now in more detail the energy dissipation mechanisms involved in the weak-solution theory. One useful technique for determining weak solutions of the one-way Eq. (9) is to apply the method of characteristics and then eliminate the multi-valued parts by inserting shocks. To find the appropriate location of the shock, Whitham (1974) proposed an ingenious method called "the equal area rule". The shock is located so that the regions cut off on either side have equal areas, as in Fig. 3. This is a consequence of mass conservation: the integral of the
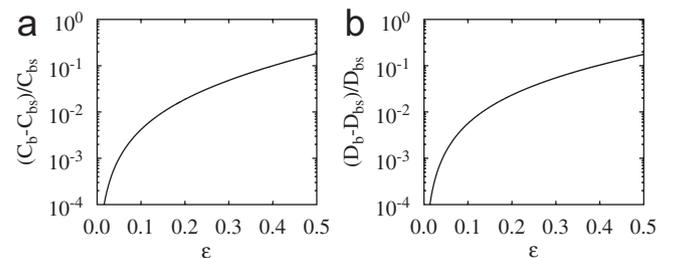

Fig. 2. Relative errors of the one-way shock velocity c_{b_s} and dissipation D_{b_s} compared to the exact shock velocity c_b and dissipation D_b, as a function of the shock strength ε. (a) $(c_b - c_{b_s})/c_{b_s}$; (b) $(D_b - D_{b_s})/D_{b_s}$.
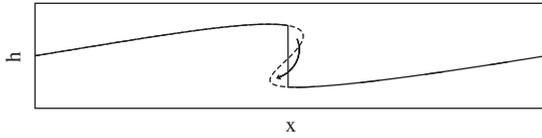
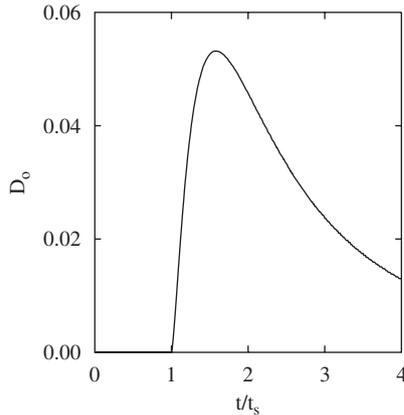Fig. 3. Multi-valued solution and equal area construction for the position of the shock.

Fig. 4. Dimensionless energy dissipation $D_a = D_{b_s}/(\rho g c_0 d_0^2)$ of a sine wave, as a function of time.

discontinuous weak solution must be the same as the area under the multi-valued solution, since both are subject to the same conservation law. It is important to emphasize again that the energy of the weak solution is not conserved in the presence of shocks. Fig. 3 clearly shows that the mass redistribution at the shock induces a decrease of the potential energy, in accordance with the actual physical wave-breaking process. Fig. 4 presents the time evolution of the energy dissipation D_{b_s} of an initial sine wave propagating on a flat bottom. Energy dissipation starts when the shock forms at $t = t_s$, increases up to $t \simeq 1.6 t_s$ and progressively decreases. This evolution, which is due to continuous broken-wave distortion, is different from those of a hydraulic jump. Indeed, the hydraulic jump reaches immediately its full strength and the energy dissipation remains constant over time. If the present discussion of dissipation processes remains qualitative, we will show in Section 5 that there is also a good quantitative agreement between theoretical and measured broken-wave energy evolution.

Let us consider now a more realistic case where periodic broken waves, of period T, propagate over a sloping beach. In that case, the onshore mass transport associated with waves propagating towards the shore is balanced by an offshore mean flow $\bar{u}$ (the time average operator is defined as $\overline{(.)} = (1/T) \int_t^{t+T} (.) \, d\tau$). Moreover, as described in the next section, broken-wave dissipation induced a wave set-up $\bar{\zeta}$. So, broken waves propagate into a water depth $\bar{h}$ with a mean current $\bar{u}$. We can consider that for a gently sloping beach wave reflexion is negligible. Indeed, in the ISZ the

wave energy of periodic waves progressively decreases shoreward due to wave breaking and then wave reflexion at the shoreline is small. So, for a gently sloping beach we can estimate that locally α^- is constant and can be evaluated using Eq. (8), $\alpha^- = u - 2c \simeq \bar{u} - 2c_m$, with $c_m = (g\bar{h})^{1/2}$. Considering that $u - 2c$ is a slow-varying function of x, which is not dependent on time, we obtain the following relation:

$$u - 2c = \bar{u} - 2\bar{c}. \tag{14}$$

With this relation, the NSW equations can be reduced to a one-way equation:

$$\frac{\partial h}{\partial t} + \frac{\partial}{\partial x}\{h(\bar{u} - 2\bar{c} + 2(gh)^{1/2})\} = 0 \tag{15}$$

with the shock condition $-c_{b_s}[h] + [q(h)] = 0$, which yields the relation

$$c_{b_s} = \bar{u} - 2\bar{c} + 2g^{1/2}\frac{h_2^{3/2} - h_1^{3/2}}{h_2 - h_1}. \tag{16}$$

We will show in Section 5 that this one-way model, associated with a wave set-up equation (see the next section), gives good results for describing the nonlinear transformation of periodic broken waves in the ISZ.

4. A wave set-up equation

Prediction of wave set-up represents an important issue of wave modelling in the surf zone. Theoretical investigations of changes in nearshore mean sea level have been initiated by Longuet-Higgins and Stewart (1964) on the basis of conservation of momentum flux. The time-averaged momentum equation provides a solution for the mean elevation $\bar{\zeta}$:

$$\frac{\partial \bar{\zeta}}{\partial x} = -\frac{1}{\rho g \bar{h}} \frac{\partial \tilde{S}}{\partial x}, \tag{17}$$

where $\tilde{S}$ is the radiation stress. Following Phillips (1977), $\tilde{S}$ can be expressed, under shallow-water wave approximations, as

$$\tilde{S} = \rho(\bar{h}\overline{\tilde{u}^2} + \tfrac{1}{2}g\overline{\tilde{\zeta}^2} + \overline{\tilde{\zeta}\tilde{u}^2} - \overline{\tilde{\zeta}\tilde{u}}^2/\bar{h}),$$

where $\tilde{\zeta} = h - \bar{h}$ is the wave elevation fluctuation and $\tilde{u} = u - \bar{u}$ the wave velocity fluctuation. In the surf zone, the wave energy decreases shoreward. The resulting changes in radiation stress lead to the wave set-up phenomenon. Consequently, Eq. (17) implicitly links wave energy dissipation and wave set-up. In this section, we will show, in the framework of NSW weak solutions, that we can derive an equation explicitly relating wave set-up and energy dissipation.

We consider periodic broken waves of period T. To derive the set-up equation we develop the expression of the

gradient $\partial \bar{\mathcal{M}}/\partial x$, where $\mathcal{M} = \frac{1}{2}u^2 + g\zeta$,

$$T\frac{\partial \bar{\mathcal{M}}}{\partial x} = \frac{\partial}{\partial x}\left(\int_t^{t+T} \mathcal{M}\,d\tau\right)$$
$$= \frac{\partial}{\partial x}\left(\int_t^{t_s^-} \mathcal{M}\,d\tau\right) + \frac{\partial}{\partial x}\left(\int_{t_s^+}^{t+T} \mathcal{M}\,d\tau\right)$$
$$= \int_t^{t_s^-}\frac{\partial \mathcal{M}}{\partial x}\,d\tau + \frac{dt_s}{dx}\mathcal{M}(t_s^-) + \int_{t_s^+}^{t+T}\frac{\partial \mathcal{M}}{\partial x}\,d\tau$$
$$- \frac{dt_s}{dx}\mathcal{M}(t_s^+), \qquad (18)$$

where $t_s(x)$ is the time at which the wavefront (or the shock) is located in x. In continuous parts of the flow, the momentum (2) is equivalent to the following equation:

$$\frac{\partial u}{\partial t} + \frac{\partial \mathcal{M}}{\partial x} = 0, \qquad (19)$$

where the friction term has been discarded. Inside intervals $[t, t_s^-]$ and $[t_s^+, t+T]$ the wave solution is continuous and so $\partial \mathcal{M}/\partial x$ in Eq. (18) can be evaluated from (19), which yields

$$T\frac{\partial \bar{\mathcal{M}}}{\partial x} = -\int_t^{t_s^-}\frac{\partial u}{\partial t}\,d\tau - \int_{t_s^+}^{t+T}\frac{\partial u}{\partial t}\,d\tau$$
$$+ \frac{1}{c_b}[\mathcal{M}] = \frac{1}{c_b}([\mathcal{M}] - c_b[u]).$$

The expression $[\mathcal{M}] - c_b[u]$ is computed using shock conditions (3) and (4):

$$[\mathcal{M}] - c_b[u] = \frac{g}{4}\frac{(h_2 - h_1)^3}{h_2 h_1} = \frac{D_b}{\rho|Q_b|}.$$

From this expression we find

$$\frac{\partial \bar{\mathcal{M}}}{\partial x} = \frac{D_{b_m}}{\rho|Q_b|},$$

where $D_{b_m} = D_b/(c_b T)$ is the mean broken-wave dissipation, and finally we obtain the new set-up equation

$$\frac{\partial \bar{\zeta}}{\partial x} = \frac{D_{b_m}}{\rho g|Q_b|} - \frac{1}{g}\frac{\partial}{\partial x}\left(\frac{1}{2}(\bar{u}^2 + \overline{\tilde{u}^2})\right). \qquad (20)$$

The main contribution for wave set-up is due to the first term on the right-hand side of Eq. (20), $\frac{D_{b_m}}{\rho g|Q_b|}$, which is related to the broken-wave energy dissipation. This term can also be written as

$$\frac{D_{b_m}}{\rho g|Q_b|} = \frac{1}{4c_b T}\frac{(h_2 - h_1)^3}{h_1 h_2}.$$

Eq. (20) is interesting from a physical point of view because, contrary to the classical theory based on radiation stresses (Longuet-Higgins and Stewart, 1964), this equation provides a simple and explicit relation between wave set-up and energy dissipation. Previous studies based on the linear wave theory (Longuet-Higgins, 1973; Dingemans et al., 1987) already showed that the wave driving force in the mean momentum equation can be expressed in function of the broken-wave energy dissipation D_{b_m}. However, to our knowledge, the present paper is the first study which explicitly states, from a nonlinear theory, the relation between wave set-up and D_{b_m}. We will show in Section 5 that Eq. (20) can represent an alternative to the classical radiation stress method for computing wave set-up in the surf zone.

5. Comparisons between model results and laboratory data

In this section, we will assess the ability of both the complete NSW model and the simplified one-way model to predict the transformation of periodic ISZ broken waves. We present comparisons between numerical solutions and spilling breaking experiments.

The main set of comparisons is based on an experiment performed by Cox (1995). This experiment was carried out in a wave flume 33 m long, 0.6 m wide and 1.5 m deep. Waves were generated on a horizontal bottom at a depth of 0.40 m, shoaled and broke on a 1:35 planar slope. The wave height at the wavemaker was $H_w = 0.115$ m and the wave period $T = 2.2$ s. Measurements of surface elevation and velocity were taken at four locations inside the ISZ (see Fig. 5). The velocities were measured with a two-component laser Doppler velocimeter (LDV).
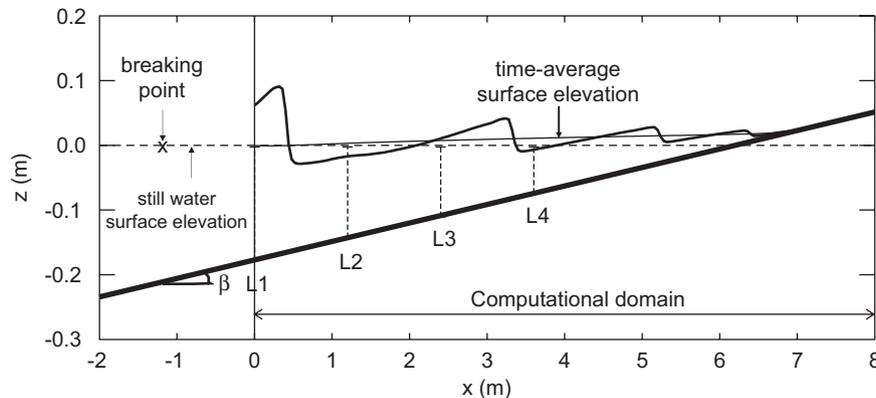

Fig. 5. Schematic view of the experimental set-up (Cox, 1995), and the computational domain. $\beta = \frac{1}{35}$, $T = 2.2$ s and $H_w = 0.115$ m. Four measurement cross-sections are located in the ISZ: L1 ($x = 0$ m, $d = 0.1771$ m); L2 ($x = 1.2$ m, $d = 0.1429$ m); L3 ($x = 2.4$ m, $d = 0.1086$ m); L4 ($x = 3.6$ m, $d = 0.0743$ m). The computational domain starts at $x = 0$ m, where the seaward boundary condition is given by time series of water depth at L1.

NSW and one-way are solved with the same shock-capturing numerical method: a TVD Mac Cormack scheme, which has been initially developed by Yee (1987) for solving the Navier Stokes compressible equations. The same method has been also implemented with success by Garcia-Navarro et al. (1992) to solve NSW equations for flood processes and hydraulic problems. The implementation of this method for solving ISZ-wave propagation is presented in Bonneton and Dupuis (2000) and Vincent et al. (2001). Efficient two-dimensional numerical schemes for the surf and swash zones can be found in Brocchini et al. (2001), Marche and Bonneton (2006) and Marche et al. (2006). The ability of our shock-capturing numerical method to converge to the weak solution of the NSW equations and then to compute the broken-wave energy dissipation is discussed in Appendix A.

The seaward boundary condition of the two models is given by time series of water depth measured at the first location L1. The computational domain was discretized by 200 nodes using a grid spacing of $\Delta x = 0.04$ m, and the models were run with a time step $\Delta t = 0.01$ s. The spatial and time steps corresponded, respectively, to $\Delta x = \lambda_0/72$ and $\Delta t = T/220$, where λ_0 is the wavelength at the seaward boundary L1.

5.1. NSW model

The initial condition of no wave motion (still water) leads to a transient period of 200 s, which is eliminated from time series presented hereafter. Previous numerical studies by Kobayashi et al. (1989) and Cox (1995) have shown that ISZ predictions were not very sensitive to the value of the friction coefficient f_r, when $0.01 \leqslant f_r \leqslant 0.05$.

In the subsequent computations we used a fixed coefficient $f_r = 0.015$.

Fig. 6 shows computed and measured time series of surface elevation at different locations inside the ISZ. The NSW model reproduces the nonlinear wave distortion and gives a good prediction of the wave height decay. The evolution towards the sawtooth shape is accurately computed by the model. Previous studies, using NSW models (Kobayashi et al., 1989; Tega and Kobayashi, 2002) or Boussinesq models (Madsen et al., 1997; Ozanne et al., 2000), showed numerical oscillations at the rear of wavefronts. We can see in Fig. 6 that our shock-capturing method prevents such numerical oscillations. The good phase agreement between computed and measured time series shows that the shock velocity c_b, given by the jump conditions (Eqs. (3) and (4)), is a good estimate of the wavefront velocity.

To emphasize this point we present in Fig. 7 a comparison between experimental wavefront positions and a wavefront trajectory computed by the NSW model. In addition, we plot in this figure trajectories computed from two other wavefront celerity expressions. The first one, $c_{b1} = ((gh_1h_2(h_1 + h_2))/(2\bar{h}^2))^{1/2}$, corresponds to the classical bore model (see Svendsen et al., 1978). The second one, $c_{b2} = 1.3(gd)^{1/2}$, is an empirical expression which is usually applied to estimate wavefront celerity (or roller celerity) in Boussinesq models (Schäffer et al., 1993). Fig. 7 shows a very good agreement between measured wavefront positions and NSW model results. We observe that trajectories computed from c_{b1} and c_{b2} are close to the measured trajectories. However, as already noticed by Bonneton (2004), the expression c_{b2} slightly overestimates the wavefront celerity and cannot be applied in the swash
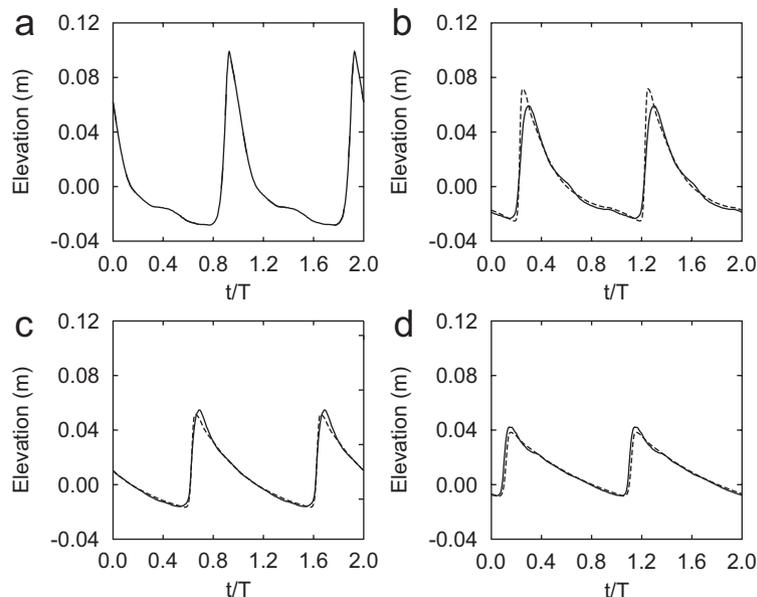

Fig. 6. Time series of surface elevation in the inner surf zone. Comparison between NSW numerical model (dashed line) and experiments by Cox (1995) (solid line). (a) L1 ($x = 0$ m, $d = 0.1771$ m); (b) L2 ($x = 1.2$ m, $d = 0.1429$ m); (c) L3 ($x = 2.4$ m, $d = 0.1086$ m); (d) L4 ($x = 3.6$ m, $d = 0.0743$ m).
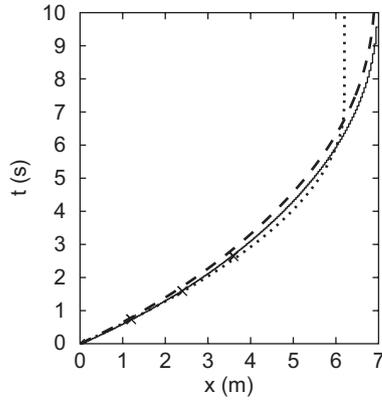
Fig. 7. Comparison between computed wavefront trajectories and experimental wavefront positions. (Solid line) NSW model; (long-dashed line) c_{b1} model; (short-dashed line) c_{b2} model; (×) experimental data from Cox (1995).
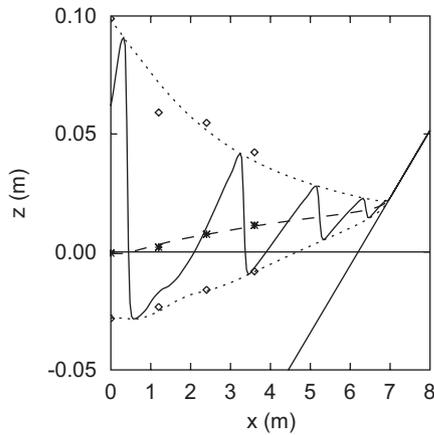

Fig. 8. Spatial evolution of wave elevation. Comparison between the NSW numerical model and experiments by Cox (1995). (Short-dashed lines) computed ζ_{min} and ζ_{max}; (long-dashed line) computed $\bar{\zeta}$; (solid line) instantaneous surface elevation at a given time t_i; (◇) measured ζ_{min} and ζ_{max}; (∗) measured $\bar{\zeta}$.

zone, and c_{b1} slightly underestimates the wavefront celerity. The ability of the NSW weak solution to predict the wavefront celerity is not limited to regular waves. Bonneton et al. (2004) have shown that the NSW model also gives an accurate prediction for the celerity of irregular waves propagating over gently sloping beaches.

Fig. 8 shows the cross-shore variations of the minimum and maximum values of wave elevation, ζ_{min} and ζ_{max}. We observe that computed ζ_{min} and ζ_{max} are in close agreement with measurements. Model–data comparisons from another spilling breaking experiment, performed by Ting and Kirby (1996), are presented in Fig. 9. This experiment is similar to Cox's experiment, with $\beta = \frac{1}{35}$, $T = 2$ s and $H_w = 0.125$ m, but the ζ-measurement spatial density is higher. Fig. 9 confirms the ability of the NSW model to predict ζ_{min} and ζ_{max} cross-shore variations, and then the wave height decay in the ISZ.

To go further in analysing the predictive capability of the NSW model, the results are compared with the phase-
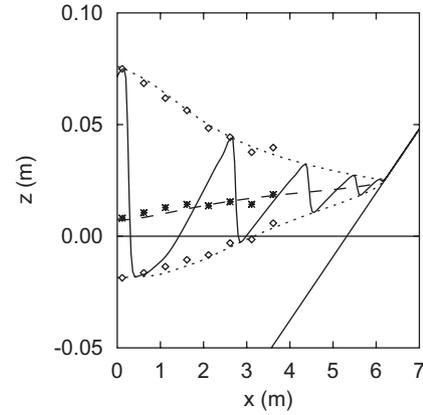

Fig. 9. Spatial evolution of wave elevation. Comparison between the NSW numerical model and experiments by Ting and Kirby (1996) ($\beta = \frac{1}{35}$, $T = 2$ s and $H_w = 0.125$ m). (Short-dashed lines) computed ζ_{min} and ζ_{max}; (long-dashed line) computed $\bar{\zeta}$; (solid line) instantaneous surface elevation; (◇) measured ζ_{min} and ζ_{max}; (∗) measured $\bar{\zeta}$.

averaged measured horizontal velocities $\langle v_1 \rangle$. The measurements are limited to the regions away from the crest because with the LDV technique it is not possible to measure velocities in the highly aerated region near the front of the breaker. Fig. 10 shows the vertical variations of $\langle v_1 \rangle$, measured at L3 for times $t = t_*$, $t = t_* + T/6$, $t = t_* + 2T/6$, $t = t_* + 3T/6$, $t = t_* + 4T/6$ and $t = t_* + 5T/6$, where t_* is the time at which the zero upcrossing of the surface elevation occurs. The solid line represents the vertical average of these velocity data, $u_m = (1/(\zeta_m + d)) \int_{-d}^{\zeta_m} \langle v_1 \rangle \, dz$, where ζ_m is the highest measurement elevation. Outside the wavefront, the wave field is characterized by a nearly vertically uniform horizontal velocity (see Figs. 10a, b, e, f) and we observe that the computed depth-averaged velocity u is a good estimate of $\langle v_1 \rangle$. Conversely, the wavefront is characterized by a strong vertical variation of $\langle v_1 \rangle$ (see Fig. 10c). In this zone, u is not representative of the velocity $\langle v_1 \rangle$ below $z = \zeta_m$ and is much greater than u_m.

Fig. 11 presents the temporal variations of computed and measured depth-averaged velocities at locations L1–L4. This figure shows that, outside the wavefront and particularly in the wave trough, u is a good estimate of u_m. Conversely, we observe that in the wavefront, u is much greater than u_m. This observation does not necessarily challenge NSW weak solutions. Indeed, we do not compare exactly the same quantities, since u_m is integrated between $z = -d$ and $z = \zeta_m$ and u is integrated over the whole depth. Moreover, we know from particle image velocimetry (PIV) observations (e.g. Govender et al., 2002) that $\langle v_1 \rangle$ is much greater in the front part of the wave crest ($z > \zeta_m$) than in the lower part. An accurate PIV determination of the depth-averaged velocity (over the whole depth) would be very useful to make clear the validity limits of NSW weak solutions in the ISZ.

For regular broken waves propagating over a low-slope beach, such as those experimentally studied by Cox (1995) and Ting and Kirby (1996), wave reflexion is small.
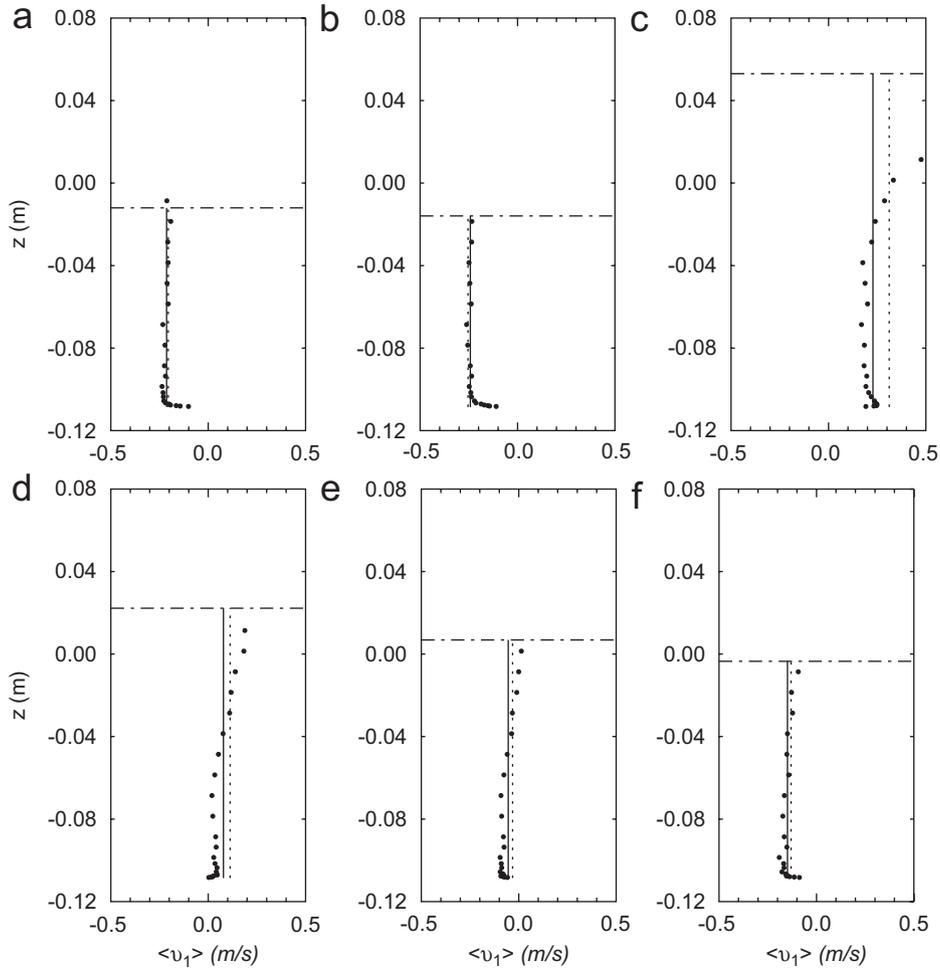
Fig. 10. Vertical structure of the phase-averaged horizontal velocity $\langle v_1 \rangle$ at L3. (•) measured velocity (Cox, 1995); (———) depth-averaged measured velocity u_{m}; (− − −) computed depth-averaged velocity u; (− · − · −) free surface position. (a) $t = t_*$; (b) $t = t_* + T/6$; (c) $t = t_* + 2T/6$; (d) $t = t_* + 3T/6$; (e) $t = t_* + 4T/6$; (f) $t = t_* + 5T/6$.

Fig. 12 presents the computed Riemann invariant $\alpha^- = u - 2c$, at a given time, as a function of x. This figure shows that α^- is approximately equal to $\bar{u} - 2\bar{c}$, except close to the shoreline. In accordance with the simple-wave solution presented in Section 3, we observe small jumps in α^- at shocks (see Eq. (11)). Nevertheless, $\bar{u} - 2\bar{c}$ is a good estimate of α^- in the ISZ. This result confirms the validity of the main hypothesis on which our one-way model is based.

5.2. One-way model

One-way solutions are determined from an iterative method, starting with $\bar{h} = d(x)$ and $\bar{u} = 0$ at the first iteration. Wave elevation fluctuations, $\tilde{\zeta} = h - \bar{h}$, and wave velocity fluctuations, $\tilde{u} = u - \bar{u}$, are computed from Eqs. (15) and (16). Then, a new estimate of $\bar{u}$ is calculated from the time-averaged mass conservation equation

$$\bar{u} = -\frac{1}{\bar{h}}\overline{\tilde{\zeta}\tilde{u}}$$

and $\bar{h} = \bar{\zeta} + d$ is given by the new set-up expression (Eq. (20)) or alternatively by the classical set-up model

(Eq. (17)). The iterative method requires about five iterations to converge to the solution.

Comparisons between one-way results and measurements by Cox (1995), Fig. 13, and Ting and Kirby (1996), Fig. 14, are presented. In these two figures, we can see that the one-way model gives a good prediction of the wave elevation field, and in particular the wave height decay and the mean set-up. Contrary to the NSW model, the one-way model slightly underestimates ζ_{min}. However, we observe in Figs. 13 and 14 that computed ζ_{min} and ζ_{max} are globally in agreement with measurements.

Figs. 13 and 14 also show that one-way solutions propagate slightly slower than NSW solutions. This observation is coherent with the simple-wave hypotheses which lead to a shock celerity $c_{\mathrm{b_s}}$ slightly smaller than the exact NSW celerity c_{b} (see Fig. 2). However, Fig. 15 shows that trajectories computed from the one-way model are close to the measured trajectories. In particular, the one-way model gives a better estimation of c_{b} than the one of the classical bore model. Bonneton (2004) has presented a more detailed analysis of ISZ broken-wave kinematics and proposed a c_{b} expression slightly more accurate than Eq. (16).
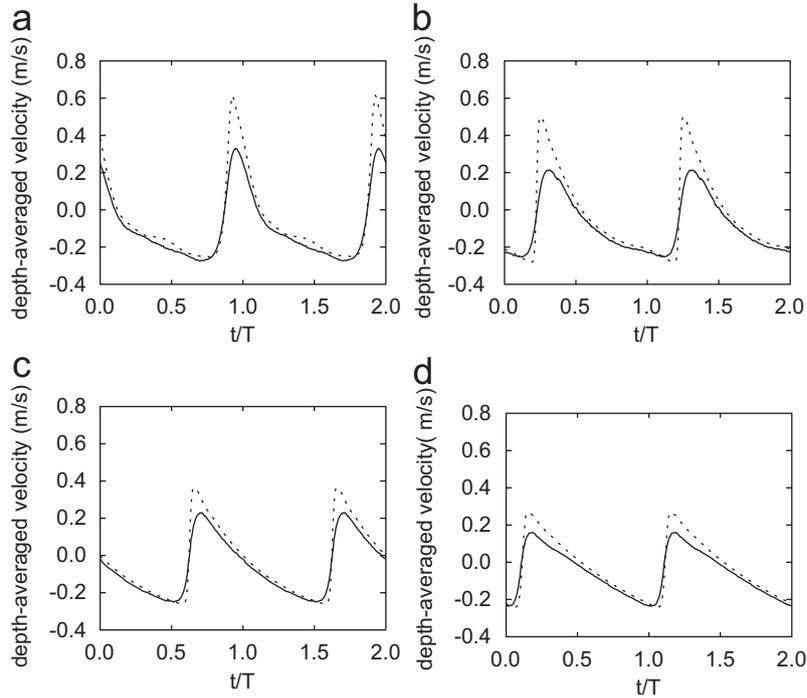
Fig. 11. Time series of depth-averaged velocity in the inner surf zone. Comparison between NSW computed velocity u (dashed line) and u_m estimated from the data of Cox (1995) (solid line). (a) L1 ($x = 0$ m, $d = 0.1771$ m); (b) L2 ($x = 1.2$ m, $d = 0.1429$ m); (c) L3 ($x = 2.4$ m, $d = 0.1086$ m); (d) L4 ($x = 3.6$ m, $d = 0.0743$ m).
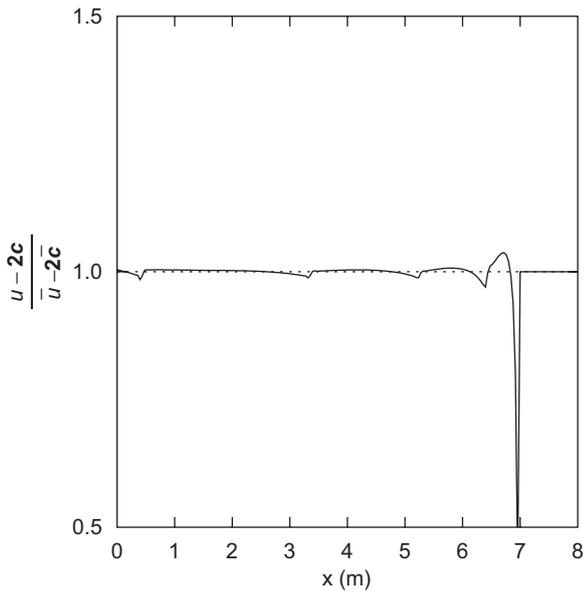

Fig. 12. NSW computed Riemann invariant $\alpha^- = u - 2c$ divided by $\bar{u} - 2\bar{c}$, at a given time t_i (see the surface elevation in Fig. 8), as a function of x.
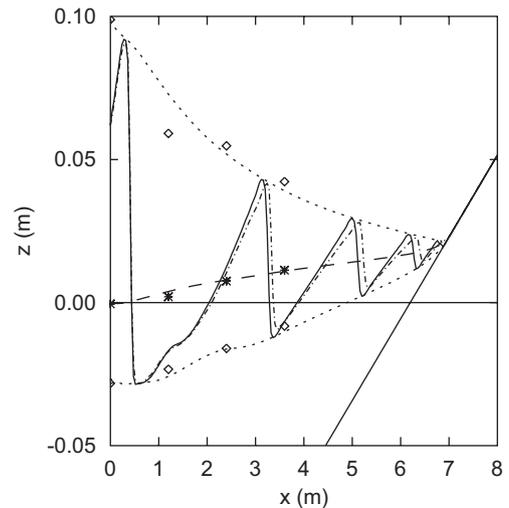

Fig. 13. Spatial evolution of wave elevation. Comparison between the one-way model and experiments by Cox (1995). (Short-dashed lines) computed ζ_{min} and ζ_{max}; (long-dashed line) computed $\bar{\zeta}$; (solid line) instantaneous surface elevation at a given time t_i; ($\diamond$) measured ζ_{min} and ζ_{max}; ($*$) measured $\bar{\zeta}$; (dot-dashed line) NSW instantaneous surface elevation at t_i.

5.3. Energy dissipation and wave set-up

We discuss now the ability of NSW and one-way solutions to predict time-averaged wave quantities such as potential energy, $E_p = \frac{1}{2}\rho g \overline{(\zeta - \bar{\zeta})^2}$, and wave set-up $\bar{\zeta}$.

Fig. 16 presents the cross-shore variation of the potential energy E_p. This figure shows that NSW and one-way

models give good predictions of the shoreward spatial decrease of E_p. Results presented in this paper about broken-wave energy decay (Figs. 8, 9, 13, 14 and 16), as well as previous numerical results by Kobayashi et al. (1989), Cox (1995), Bonneton (2003) and Bonneton et al. (2004), seem to indicate that the theoretical energy
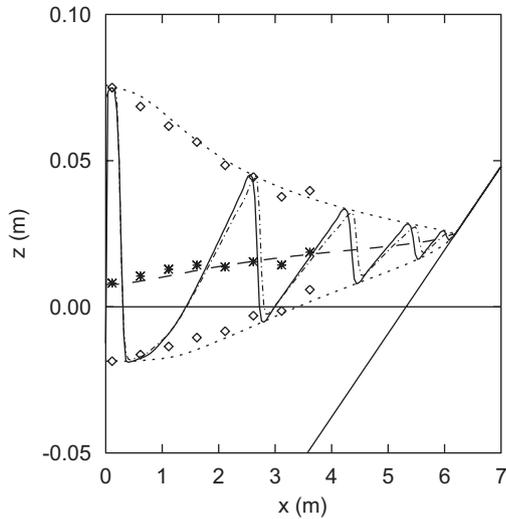
Fig. 14. Spatial evolution of wave elevation. Comparison between the one-way model and experiments by Ting and Kirby (1996) ($\beta = \frac{1}{35}$, $T = 2\,\text{s}$ and $H_w = 0.125\,\text{m}$). (Short-dashed lines) computed ζ_{min} and ζ_{max}; (long-dashed line) computed $\bar{\zeta}$; (solid line) instantaneous surface elevation; ($\diamond$) measured ζ_{min} and ζ_{max}; ($*$) measured $\bar{\zeta}$; (dot-dashed line) NSW instantaneous surface elevation.
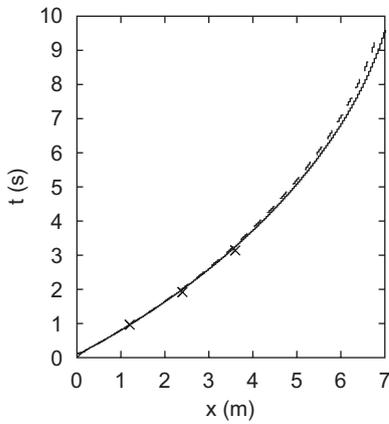

Fig. 15. Comparison between computed wavefront trajectories and experimental wavefront positions. (Solid line) NSW model; (dashed line) one-way model; ($\times$) experimental data from Cox (1995).
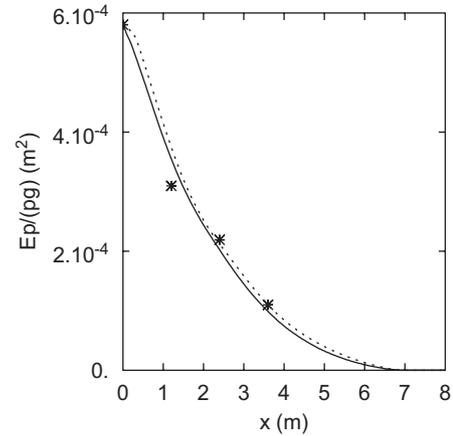

Fig. 16. Measured and computed cross-shore variations of the potential energy E_p. ($*$) Cox (1995) experiment; (solid line) NSW model; (dashed line) one-way model.
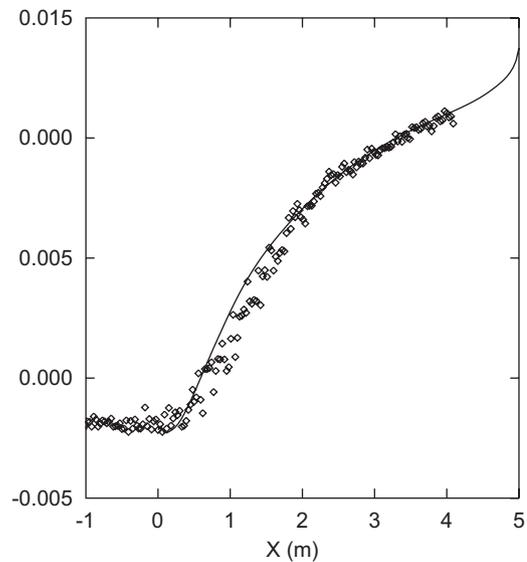

Fig. 17. Cross-shore variations of the wave set-up. Comparisons between NSW numerical model (solid line) and experiments by Buhr-Hansen and Svendsen (1979) ($\diamond$). $\beta = \frac{1}{34.26}$, $T = 1.452\,\text{s}$ and $H_w = 0.0943\,\text{m}$.

dissipation D_b (Eq. (5)), or its one-way formulation D_{b_s} (Eq. (13)), represents good estimates of the actual energy dissipation.

Fig. 17 presents the measured and computed variations of the time-averaged free surface elevation $\bar{\zeta}$, for a third spilling breaking experiment, performed by Buhr-Hansen and Svendsen (1979). We observe in the three Figs. 8, 9 and 17 that the set-up $\bar{\zeta}$ is accurately predicted by the NSW model. This shows that the NSW weak solution represents an appropriate model for describing the ISZ set-up.

As shown in Figs. 13, 14 and 18, the wave set-up is also well predicted by the one-way shock-wave model. Figure 18 shows that the new set-up equation (Eq. (20)) gives similar results than the classical set-up equation (Eq. (17)) based on radiation stress. The new set-up equation, which directly relies on $\partial \bar{\zeta}/\partial x$ and jump characteristics (h_1, h_2 and

c_b), can represent an useful alternative to the classical set-up formulation.

6. Conclusion

In this paper, we have analysed the ability of the time-dependent NSW equations to predict periodic broken-wave transformation in the ISZ. This analysis was based on the weak-solution theory for conservative equations, which allows to predict global wave evolution without a detailed description of small-scale processes located at wavefronts. We have derived a new one-way model (Eqs. (15) and (16)), which applies to the transformation of non-reflective periodic broken waves on gently sloping beaches. Even if numerical solutions of the complete NSW equations can be computed, our simplified one-way approach is useful because it gives us a better understanding of wave
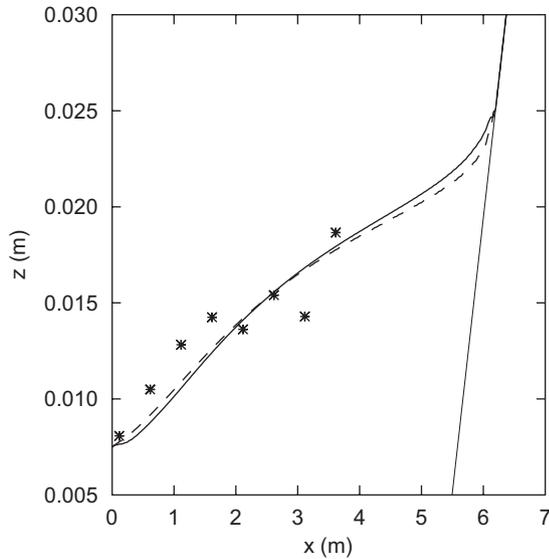
Fig. 18. Cross-shore variations of the wave set-up computed with the one-way model. (Dashed line) new set-up expression, Eq. (20); (solid line) classical set-up model, Eq. (17); (∗) Ting and Kirby (1996) experiment.

distortion and energy dissipation in the ISZ. Moreover, this one-way model can be useful to provide breaking-wave parameterizations (in particular broken-wave celerity expression) in both time-averaged wave models and time-dependent Boussinesq-type models.

In the theoretical framework of NSW weak solutions we have also derived a new wave set-up equation (Eq. (20)). This equation is interesting from a physical point of view because, contrary to the classical theory based on radiation stresses, it provides a simple and explicit relation between wave set-up and energy dissipation. We have shown in Section 5 that this equation can represent an alternative to the classical radiation stress method for computing wave set-up in the surf zone.

A detailed comparison with spilling wave-breaking experiments has shown that both NSW and one-way solutions compare very well with experimental data. Both models reproduce the nonlinear wave distortion leading to the sawtooth shape, and give a good prediction of broken-wave celerity c_b, wave height decay and time-averaged quantities such as wave set-up.

Acknowledgements

Appendix A. Numerical estimation of the broken-wave energy dissipation

The objective of this Appendix is to show the ability of our shock-capturing numerical method to converge to the

weak solution of the NSW equations and then to compute the broken-wave energy dissipation. To do that, we present a comparison between numerical and analytical NSW solutions. Fig. 19 shows a comparison between the NSW numerical solution of the initial sine-wave transformation on a flat bottom and the one-way solution described in Section 3. The process of wave distortion, leading to the formation of a sawtooth shape profile, is correctly computed by the model. Until the shock forms at $t = t_s$,
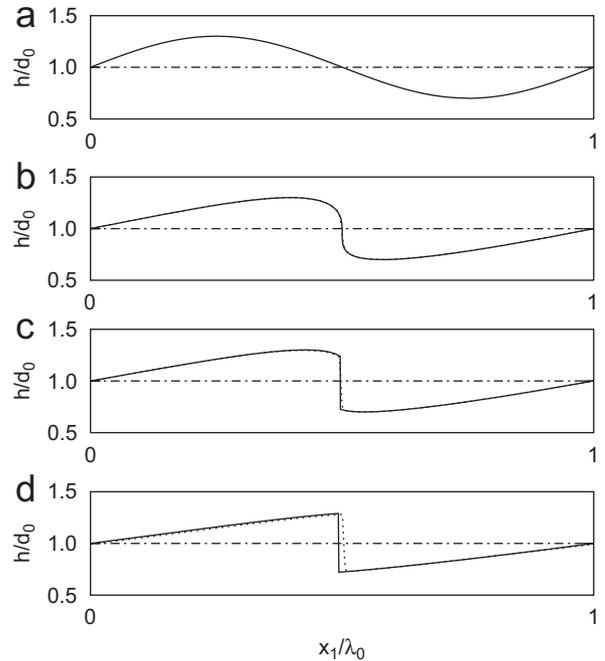

Fig. 19. Comparison between analytical one-way solution (solid line) and numerical solution (short-dashed line) of the initial sine-wave ($\varepsilon_0 = 0.3$) transformation in the moving coordinate system $x_1 = x - c_0 t$. Numerical parameters: $\Delta x/\lambda_0 = 2 \times 10^{-3}$, $\Delta t/(c_0\lambda_0) = 6.4 \times 10^{-5}$. (a) $t/t_s = 0$; (b) $t/t_s = 1$; (c) $t/t_s = 1.2$; (d) $t/t_s = 2$.
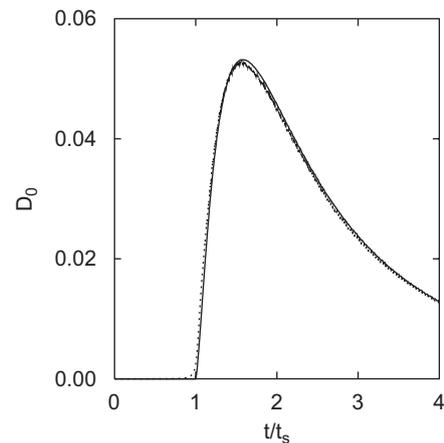

Fig. 20. Time evolution of the dimensionless energy dissipation $D_a = D_{b_s}/(\rho g c_0 d_0^2)$. Comparison between analytical one-way solution (solid line) and numerical solution (short-dashed line) of the initial sine-wave ($\varepsilon_0 = 0.3$) transformation. Numerical parameters: $\Delta x/\lambda_0 = 2 \times 10^{-3}$, $\Delta t/(c_0\lambda_0) = 6.4 \times 10^{-5}$.
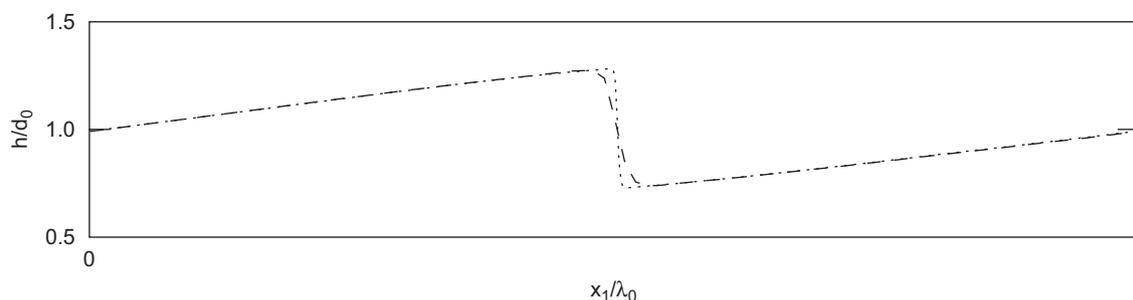
Fig. 21. Numerical solutions of the initial sine-wave ($\varepsilon_0 = 0.3$) transformation in the moving coordinate system $x_1 = x - c_0 t$, at $t/t_s = 2$ with $\Delta t/(c_0\lambda_0) = 6.4 \times 10^{-5}$. (Dashed line) $\Delta x/\lambda_0 = 2 \times 10^{-3}$; (short-dashed line) $\Delta x/\lambda_0 = 10^{-2}$.

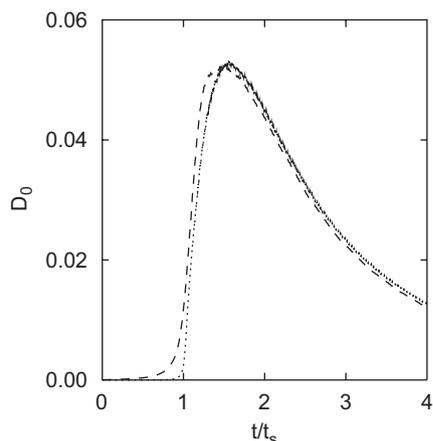
Fig. 22. Time evolution of the dimensionless energy dissipation $D_a = D_{b_s}/(\rho g c_0 d_0^2)$, for two different spatial resolutions. (Dashed line) $\Delta x/\lambda_0 = 2 \times 10^{-3}$; (short-dashed line) $\Delta x/\lambda_0 = 10^{-2}$.

there is no distinguishable difference between analytical and computed solutions (see Fig. 19b). After the shock formation (see Figs. 19c, d), we notice that the NSW computed wavefront propagates slightly faster than the one-way solution. This is coherent with the simple-wave hypotheses which lead to a shock velocity c_{b_s} slightly smaller than the exact NSW shock velocity c_b (see Fig. 2a). Fig. 20 shows that energy dissipation computed by the shock-capturing method is in close agreement with the analytical one-way solution.

To assess the effect of spatial resolution on wave solution, numerical simulations performed with two different mesh sizes are presented in Fig. 21. The two solutions are similar, except at the wavefront where the lower resolution provides, of course, a wider front. This figure shows that the computed shock-wave kinematics is, to a great extent, independent on the spatial resolution. Time evolution of energy dissipation computed with two different mesh sizes is presented in Fig. 22. We can see that the energy dissipation is weakly dependent on the resolution.

In conclusion, if the spatial mesh size is sufficiently small to describe the wavefront, the numerical solution given by our TVD shock-capturing method is practically indepen- dent of the spatial resolution and converges to the NSW weak solution.

References

Battjes, J.A., Janssen, J.P.F.M., 1978. Energy loss and setup due to breaking of random waves. In: Proceedings of the International Conference on Coastal Engineering, ASCE, pp. 569–587.

Bonneton, P., 2001. A note on wave propagation in the inner surf zone. Comptes Rendus de l'Academie des Sciences Paris Série II b 329, 27–33.

Bonneton, P., 2003. Dynamique non-linéaire des vagues en zone de surf interne. Revue Française de Génie Civil 7, 1061–1076 (numéro spécial "Génie-Côtier").

Bonneton, P., 2004. Wave celerity in the inner surf zone. In: Proceedings of the 29th International Conference on Coastal Engineering, vol. 1, pp. 392–401.

Bonneton, P., Dupuis, H., 2000. Transformation of irregular waves in the inner surf zone. Proceedings of the 27th International Conference on Coastal Engineering. vol. 1, pp. 745–754.

Bonneton, P., Marieu, V., Dupuis, H., Sénéchal, N., Castelle, B., 2004. Wave transformation and energy dissipation in the surf zone: comparison between a non-linear model and field data. Journal of Coastal Research SI 39, 329–333.

Bowen, A.J., Inman, D.L., Simmons, V.P., 1968. Wave setdown and setup. Journal of Geophysical Research 73, 2569–2577.

Brocchini, M., Bernetti, R., Mancinelli, A., Albertini, G., 2001. An efficient solver for nearshore flows based on the WAF method. Coastal Engineering 43, 105–129.

Buhr-Hansen, J., Svendsen, I.A., 1979. Regular waves in shoaling water experimental data. Series Paper No. 21, ISVA, Technical University of Denmark, Lyngby.

Cox, D.T., 1995. Experimental and numerical modelling of surf zone hydrodynamics. Ph.D. Dissertation, University of Delaware, Newark.

Dingemans, M.W., Radder, A.C., De Vriend, H.J., 1987. Computation of the driving forces of wave-induced currents. Coastal Engineering 11, 539–563.

Galvin, C.J., 1968. Breaker type classification on three laboratory beaches. Journal of Geophysical Research 73, 3651–3659.

Garcia-Navarro, P., Alcrudo, F., Saviron, J.M., 1992. 1-D open channel flow simulation using TVD-McCormack scheme. Journal of Hydraulic Engineering 118, 1359–1372.

Govender, K., Mocke, G.P., Alport, M.J., 2002. Video-imaged surf zone wave and roller structures and flow fields. Journal of Geophysical Research 107, 3072–3093.

Hibbert, S., Peregrine, D.H., 1979. Surf and run-up on a beach: a uniform bore. Journal of Fluid Mechanics 95, 323–345.

Ho, D.V., Meyer, R.E., 1962. Climb of a bore on a beach. Part 1: uniform beach slope. Journal of Fluid Mechanics 14, 305–318.

Keller, H.B., Levine, D.A., Whitham, G.B., 1960. Motion of a bore over a sloping beach. Journal of Fluid Mechanics 7, 302–316.

Kobayashi, N., DeSilva, G.S., Watson, K.D., 1989. Wave transformation and swash oscillation on gentle and steep slopes. Journal of Geophysical Research 94 (C1), 951–966.

Kobayashi, N., Cox, D.T., Wurjanto, A., 1990. Irregular wave reflection and run-up on rough impermeable slopes. Journal of Waterway, Port, Coastal, and Ocean Engineering 116, 708–728.

Le Méhauté, B., 1962. On the non-saturated breaker theory and the wave run-up. In: Proceedings of the Eighth Coastal Engineering Conference, pp. 77–92.

Liu, P.L.-F., Synolakis, C.E., Yeh, H.H., 1991. Report on the international workshop on long-wave run-up. Journal of Fluid Mechanics 229, 675–688.

Longuet-Higgins, M.S., 1973. The mechanics of the surfzone. In: Proceedings of the 13th International Congress of Theoretical and Applied Mechanics, Springer, Moscow, pp. 213–228.

Longuet-Higgins, M.S., Stewart, R.W., 1964. Radiation stress in water waves, a physical discussion with application. Deep-Sea Research 11, 529–563.

Madsen, P.A., Sorensen, O.R., Schäffer, H.A., 1997. Surf zone dynamics simulated by a Boussinesq type model. Part I. Model description and cross-shore motion of regular waves. Coastal Engineering 32, 255–287.

Marche, F., Bonneton, P., 2006. A simple and efficient well-balanced model for 2DH bore propagation and run-up over sloping beach. In: Proceedings of the 30th International Conference on Coastal Engineering.

Marche, F., Bonneton, P., Fabrie, P., Seguin, N., 2006. Evaluation of well-balanced bore-capturing schemes for 2D wetting and drying processes. International Journal for Numerical Methods in Fluids, in press.

Ozanne, F., Chadwick, A.J., Huntley, D.A., Simmonds, D.J., Lawrence, J., 2000. Velocity predictions for shoaling and breaking waves with a Boussinesq-type model. Coastal Engineering 41, 361–397.

Peronnard, C., Hamm, L., 1995. Database waves and associated currents for coastal profile modelling (release 1.1). Report SOGREAH No. 52184R6, prepared for G8M Coastal Morphodynamics European Project No. MS2-CT92-0027, Grenoble, France.

Phillips, O.M., 1977. The Dynamics of the Upper Ocean, second ed. Cambridge University Press, Cambridge.

Raubenheimer, B., Guza, R.T., Elgar, S., 1996. Wave transformation across the inner surf zone. Journal of Geophysical Research 101 (C10), 25589–25597.

Schäffer, H.A., Madsen, P.A., Deigaard, R., 1993. A Boussinesq model for waves breaking in shallow water. Coastal Engineering 20, 185–202.

Sénéchal, N., Dupuis, H., Bonneton, P., Howa, H., Pedreros, R., 2001. Observation of irregular wave transformation in the surf zone over a gently slopping sandy beach. Oceanologica Acta 24 (6), 545–556.

Stoker, J.J., 1957. Water Waves. Interscience, New York.

Svendsen, I.A., Madsen, P.A., Hansen, J.B., 1978. Wave characteristics in the surf zone. In: Proceedings of the 16th Coastal Engineering Conference, pp. 520–539.

Svendsen, I.A., Qin, W., Ebersole, B.A., 2003. Modelling waves and currents at the LSTF and other laboratory facilities. Coastal Engineering 50, 19–45.

Tega, Y., Kobayashi, N., 2002. Sediment transport in wave uprush and downrush on swash zone. In: Proceedings of the 28th Coastal Engineering Conference, pp. 993–1005.

Thornton, E.B., Guza, R.T., 1982. Energy saturation and phase speeds measured on a natural beach. Journal of Geophysical Research 87, 9499–9508.

Ting, F.C.K., Kirby, J.T., 1996. Dynamics of surf-zone turbulence in a spilling breaker. Coastal Engineering 27, 131–160.

Vincent, S., Bonneton, P., Caltagirone, J-P., 2001. Numerical modelling of bore propagation and run-up on sloping beaches using a MacCormack TVD scheme. Journal of Hydraulic Research 39, 41–49.

Whitham, G.B., 1958. On the propagation of shock waves through regions of non-uniform area or flow. Journal of Fluid Mechanics 4, 337–360.

Whitham, G.B., 1974. Linear and Nonlinear Waves. Wiley-Interscience, New York.

Yee, H.C., 1987. Upwind and symmetric shock-capturing schemes. NASA Technical Memorandum, 89464.